

Correlated Λd pairs from the $K_{stop}^- A \rightarrow \Lambda d A'$ reaction

FINUDA Collaboration

M. Agnello^a, G. Beer^b, L. Benussi^c, M. Bertani^c,
 H.C. Bhang^d, S. Bianco^c, G. Bonomi^v, E. Botta^e,
 M. Bregant^f, T. Bressani^e, S. Bufalino^e, L. Busso^g, D. Calvo^h,
 P. Camerini^f, M. Caponeroⁱ, P. Cerello^h, B. Dalena^j,
 F. De Mori^e, G. D'Erasmus^j, D. Di Santo^j, R. Donà^k, D. Elia^j,
 F. L. Fabbri^c, D. Faso^g, A. Feliciello^h, A. Filippi^h,
 V. Filippini^{l,2}, R. Fini^j, M. E. Fiore^j, H. Fujioka^m,
 P. Gianotti^c, N. Grionⁿ, O. Hartmann^c, A. Krasnoperov^o,
 V. Lucherini^c, V. Lenti^j, V. Manzari^u, S. Marcello^e,
 T. Maruta^m, N. Mirfakhrai^p, O. Morra^q, T. Nagae^r, A. Olin^s,
 H. Ota^t, E. Pace^c, M. Pallotta^c, M. Palomba^j, A. Pantaleo^u,
 A. Panzarasa^l, V. Paticchio^u, S. Piano^{n,1}, F. Pompili^c,
 R. Rui^f, G. Simonetti^j, H. So^d, V. Tereshchenko^o,
 S. Tomassini^c, A. Toyoda^r, R. Wheadon^h, A. Zenoni^v

^a*Dip. di Fisica Politecnico di Torino, Corso Duca degli Abruzzi Torino, Italy, and INFN Sez. di Torino, via P. Giuria 1 Torino, Italy*

^b*University of Victoria, Finnerty Rd., Victoria, Canada*

^c*Laboratori Nazionali di Frascati dell'INFN, via E. Fermi 40 Frascati, Italy*

^d*Dep. of Physics, Seoul National Univ., 151-742 Seoul, South Korea*

^e*Dipartimento di Fisica Sperimentale, Università di Torino, via P. Giuria 1 Torino, Italy, and INFN Sez. di Torino, via P. Giuria 1 Torino, Italy*

^f*Dip. di Fisica Univ. di Trieste, via Valerio 2 Trieste, Italy and INFN, Sez. di Trieste, via Valerio 2 Trieste, Italy*

^g*Dipartimento di Fisica Generale, Università di Torino, via P. Giuria 1 Torino, Italy, and INFN Sez. di Torino, via P. Giuria 1 Torino, Italy*

^h*INFN Sez. di Torino, via P. Giuria 1 Torino, Italy*

ⁱ*ENEA, Frascati, Italy*

^j*Dip. di Fisica Univ. di Bari, via Amendola 179 Bari, Italy and INFN Sez. di Bari, via Amendola 179 Bari, Italy*

^k*Dipartimento di Fisica, Università di Bologna, via Irnerio 46, Bologna, Italy and
INFN, Sezione di Bologna, via Irnerio 46, Bologna, Italy*

^l*INFN Sez. di Pavia, via Bassi 6 Pavia, Italy*

^m*Dep. of Physics Univ. of Tokyo, Bunkyo Tokyo 113-0033, Japan*

ⁿ*INFN, Sez. di Trieste, via Valerio 2 Trieste, Italy*

^o*Joint Institute for Nuclear Research (JINR), Dubna, Russia*

^p*Dep of Physics Shahid Beheshti Univ., 19834 Teheran, Iran*

^q*INAF-IFSI Sez. di Torino, C.so Fiume, Torino, Italy and INFN Sez. di Torino,
via P. Giuria 1 Torino, Italy*

^r*High Energy Accelerator Research Organization (KEK), Tsukuba, Ibaraki
305-0801, Japan*

^s*TRIUMF, 4004 Wesbrook Mall, Vancouver BC V6T 2A3, Canada*

^t*RIKEN, Wako, Saitama 351-0198, Japan*

^u*INFN Sez. di Bari, via Amendola 179 Bari, Italy*

^v*Dip. di Ingegneria Meccanica e Industriale, Università di Brescia, via Branze 38
Brescia, Italy and INFN Sez. di Pavia, via Bassi 6 Pavia, Italy*

Abstract: Correlated Λd pairs emitted after the absorption of negative kaons at rest $K_{stop}^- A \rightarrow \Lambda d A'$ in light nuclei ${}^6\text{Li}$ and ${}^{12}\text{C}$ are studied. Λ -hyperons and deuterons are found to be preferentially emitted in opposite directions. The Λd invariant mass spectrum of ${}^6\text{Li}$ shows a bump whose mass is 3251 ± 6 MeV/c². The bump mass (binding energy), width and yield are reported. The appearance of a bump is discussed in the realm of the $[\bar{K}3N]$ clustering process in nuclei. The experiment was performed with the FINUDA spectrometer at DAΦNE (LNF).

PACS:21.45.+v, 21.80.+a 25.80.Nv

I. INTRODUCTION

In this letter we investigate the invariant mass spectra of correlated Λd pairs, which are produced by the kaon absorption reaction $K_{stop}^- A \rightarrow \Lambda d A'$. The nuclei (A) examined are ${}^6\text{Li}$ and ${}^{12}\text{C}$ and the Λ -hyperon and deuteron are the reconstructed particles in the reaction final state. The present study follows an earlier Λp survey on light and medium-light nuclei made by the FINUDA collaboration [1], which supported the view that negative kaons gather nucleons to form bound systems; i.e., $K_{stop}^- pp \rightarrow [K^- pp] \rightarrow \Lambda p$. The present discussion about the dynamics of $[\bar{K}3N]$ clusters in A is pursued by studying the $A(K_{stop}^-, \Lambda d)A'$ reaction channel.

¹ corresponding author. E-mail: stefano.piano@ts.infn.it; Fax: ++39.040.5583350.

² deceased

A $[\overline{K}3N]$ cluster was found in the course of a search for neutrons emitted from the $K_{stop}^- {}^4He \rightarrow nA'$ absorption reaction, where A' is the residual nucleus [2]. These neutron data, which result from semi-inclusive measurements, show a bump in the excitation spectrum in the range 450-500 MeV/c. The resulting missing mass spectrum also has this bump interpreted by the authors as a $[\overline{K}3N]$ bound state, named the *strange tribaryon* S^+ [2]. The measured S^+ mass and width are 3140.5 MeV/c² and <21.6 MeV/c², respectively. The theoretical explanation of the $S^+(3140)$ as the distinctive pattern of a deeply-bound \overline{K} state [3] was contentious; in fact, theory requires an uncommonly deep potential with a small imaginary part to reproduce the data [4]. The $[\overline{K}3N]$ core density, which may be as high as 5 times nuclear density, was also contentious.

Experimental investigation of the existence of K^- -bound nuclear states began several years ago [1,2]. Theoretical studies were started earlier. The reality of these states was never disputed, although the values of their binding energy and width strongly depend on both the model and the parameters used. For example, the \overline{K} -nuclear potential is predicted to range from deep (150-200 MeV [5]) to shallow (50-60 MeV [6]). Widths, also predicted to vary, are critical for the detection of K^- -nuclear states.

Proof of the existence of strange heavy baryons or the actuality of nuclear \overline{K} bound states, whether discrete or not, cannot simply rely on (semi-)inclusive measurements. In fact, the erroneous interpretation of a bump observed in the energy distribution of protons from the $K_{stop}^- {}^4He \rightarrow pA'$ reaction led to prediction of the neutral strange tribaryon $A' \equiv S^0(3115)$ [7]. The data discussed in this article exploit the capability of the FINUDA spectrometer to fully reconstruct the $A(K_{stop}^-, \Lambda d)A'$ reaction with A' undetected, thereby yielding a quasi-complete kinematic picture of the detected events.

II. THE EXPERIMENTAL METHOD

The search for $[\overline{K}3N]$ clusters makes use of the absorption reaction $K_{stop}^- A \rightarrow \Lambda(1116)dA'$, where A is either 6Li or ${}^{12}C$ and A' is a system of $(A-3)$ nucleons not necessarily bound. The experimental method is briefly explained in this letter; however, further details can be found in Refs. [8,9,10].

At the DAΦNE collider at LNF, 510 MeV electron/positron collisions produce 16.1 ± 1.5 MeV kaons as a by-product of the multistep process $e^+e^- \rightarrow \Phi(1020) \rightarrow K^+K^-$ (B.R.~50%). The kaons slow down as they traverse some of the sensitive layers of FINUDA until they come to rest within solid targets as thin as 0.213 g/cm² for 6Li and 0.295 g/cm² for ${}^{12}C$. Both kaons and their decay or reaction products, μ 's, π 's, p 's and d 's, are analyzed in FINUDA. The magnetic spectrometer has cylindrical geometry, centered on the $\Phi(1020)$ -production volume. The magnetic field was set at 1.0 T. The innermost sensitive layer, (TOFINO) [11], is a segmented detector made of plastic scintillator, which is optimized for starting the time-of-flight system. TOFINO is followed by two layers of double-sided silicon strip detectors, which

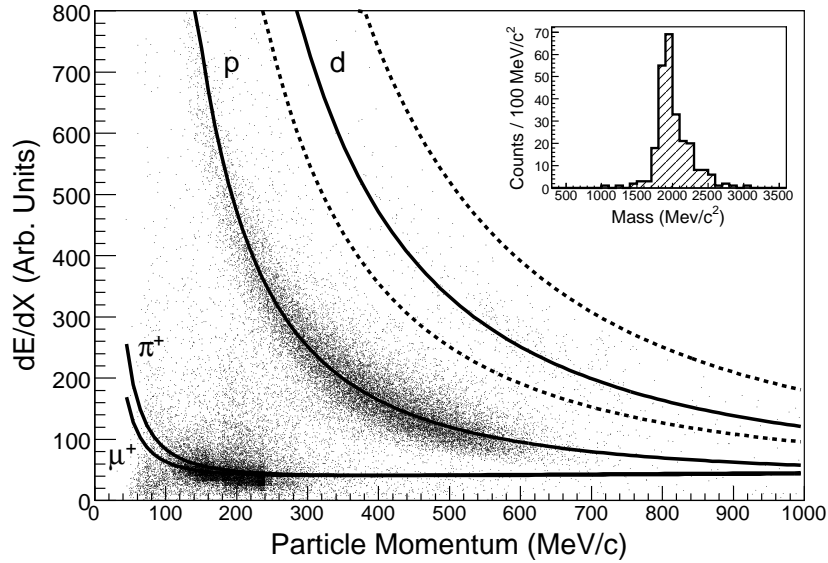


Fig. 1. dE/dx vs momentum diffusion plot of μ 's, π 's, p 's and d 's. Full lines, Bethe-Bloch functions. The dashed lines delimit the full-width-at-tenth-maximum region of deuterons. Inset, mass distribution of the particles falling into the deuteron region. More details are given in the text.

are used for both localization and identification of charged particles (ISIM and OSIM)[12]. The (eight) targets are accommodated between ISIM and OSIM. Next, two layers of drift chambers (LMDC) identify and locate charged particles [13]. A stereo-arrangement of straw tubes is the last sensitive tracking layer located within the magnetic field (ST) [14]. This stereo device is the last layer used for particle localization. The outermost layer of FINUDA consists of a segmented detector, TOFONE, made of rectangular slabs of plastic scintillator [15]. TOFONE is designed as the stop for the FINUDA time-of-flight measurements and also measures the energy released by charged particles.

The charged particles involved in the absorption (or decay) process are mass-identified by specific energy deposit (dE/dx) in some of the layers of the spectrometer. In fact, a coherent response from a minimum of 3 dE/dx layers is required to identify (ID) a particle as a pion, a proton or a deuteron. Fig. 1 shows the dE/dx -response of OSIM (scatterplots) and the Bethe-Bloch functions (full lines) for μ 's, π 's, p 's and d 's, as a function of the particle momenta. These particles, the result of minimum-bias triggers, are not related to any specific kaon absorption reaction channel. The dashed lines define the deuteron region, which is chosen by means of a full-width-at-tenth-maximum (FWTM) criterion. To check the validity of this criterion, the mass of the particles falling into the deuteron region is independently determined by measuring their time-of-flight between TOFINO and TOFONE. The particle mass distribution is shown in the inset of Fig. 1. It appears as a peak centered at a mass value of ≈ 1880 MeV with a FWTM strength that accounts for more than 96% of the total strength.

The initial selection of π^-pd events relies on the particle ID of FINUDA. Such events are

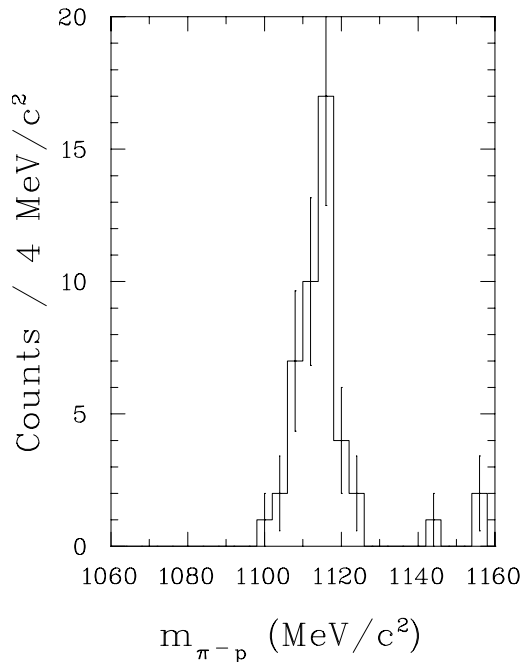


Fig. 2. Invariant mass distribution of π^-p pairs for ${}^6\text{Li}$. The π^-p events forming the histogram are in coincidence with deuterons.

seldom accompanied by other charged particles. Once a π^-pd event is identified, the $\Lambda(1116)d$ channel is entirely reconstructed as well as the track of the stopped negative kaons. The topology of the $\Lambda(\rightarrow p\pi^-)d$ events, when combined with the selective particle ID of FINUDA, provides distributions nearly free from accidental as well as combinatorial background. As an example, Fig. 2 shows the m_{π^-p} distribution of ${}^6\text{Li}$. The uniform distribution of background events over the mass ranges 1080-1102 and 1128-1150 MeV around the Λ peak makes it possible to assess the number of such events inside the peak itself. The background events are 2.2 ± 0.9 out of a total of 46 Λ events, which were produced by $3.38 \times 10^6 K_{stop}^-$. Λ hyperons are detected from 140 MeV/c (threshold) up to 700 MeV/c, whereas deuterons from the Λd channel are analyzed starting from 300 MeV/c (threshold) up to momenta of about 800 MeV/c. Both Λ 's and d 's are measured with a resolution $\Delta p/p < 2\%$. Opening angles in the full range from $0^\circ \leq \Theta_{\Lambda d} < 180^\circ$ were measured. Spectra are corrected for the spectrometer acceptance, which also includes the event reconstruction efficiency. The acceptance for the Λd invariant mass ($m_{\Lambda d}$) increases nearly linearly between 3100 and about 3340 MeV/c² (curve not shown). The error bars reflect the systematic uncertainty due to the evaluation of the FINUDA acceptance. The dominant statistical uncertainty is summed in quadrature with this systematic uncertainty in the following analysis, and overall error bars are reported in Figs. 3, 4 and 5.

III. THE RESULTS

Fig. 3 shows the Λd invariant mass for the ${}^6\text{Li}$ target. We observed a bump at $m_{\Lambda d} \sim 3250$ MeV/c² and the purpose of the present analysis is to try to understand its nature. To this end,

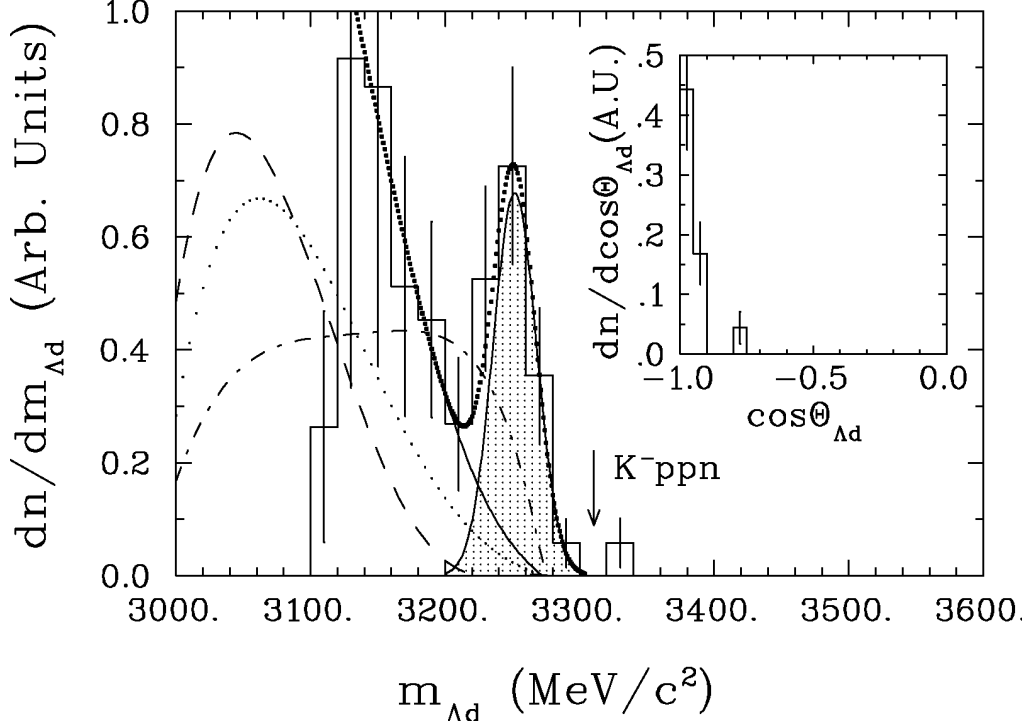


Fig. 3. Invariant mass distribution of Λd pairs from the ${}^6\text{Li}(K_{stop}^-, \Lambda d)3N$ reaction (full-line histogram). Dash-line, small-dot-line and dash-dot-line curves, phase space simulations of the (1) $\Lambda d n n p$, (2) $\Lambda d n d$ and (3) $\Lambda d t$ reaction channels, respectively. Big-dot-line curve, data fitted with a linear combination of channels (1), (2) and (3) and a Gaussian function (gray-fill curve). Full-line curve, simulated background. The arrow indicates the overall mass of the unbound $K^- p p n$ system. Inset, $\cos\Theta_{\Lambda d}$ distribution of the events populating the bump at 3250 MeV/c².

the $m_{\Lambda d}$ distribution (thin-line histogram) is compared with the phase-space behavior of Λd pairs from the $K_{stop}^- {}^6\text{Li} \rightarrow \Lambda d 3N$ absorption reaction. The following three reaction channels were investigated: (1) $\Lambda d n n p$, (2) $\Lambda d n d$ and (3) $\Lambda d t$. The Λd pairs from (1) (dashed curve) have an invariant mass distribution which shows negligible strength above 3210 MeV/c²; therefore, these pairs barely contribute to the bump at 3250 MeV/c². The small-dot curve depicts the $m_{\Lambda d}$ phase space of channel (2). The mass distribution of channel (3) (dot-dash curve) also extends through the mass range of the data. These three distributions were arbitrarily normalized to the data. The phase space simulations indicate that the $m_{\Lambda d}$ threshold is slightly below 3000 MeV/c², a mass limit which cannot be probed by FINUDA. This is due to the low acceptance of the apparatus below 3100 MeV/c² combined with poor statistics. Consequently, the peak shape of the spectrum at ≈ 3140 MeV/c² may be an artifact.

Σ^0 hyperons may also feed the Λd channel via $\Sigma^0 \rightarrow \Lambda \gamma$ decays. In this case, the energy taken away by the γ rays ($T_\gamma=74$ MeV) shifts the $m_{\Lambda d}$ endpoints of channels (1), (2) and (3) lower, rendering their contribution to the $m_{\Lambda d}$ distribution above 3100 MeV/c² less significant. In addition, the branching ratios for K_{stop}^- in ${}^4\text{He}$ are 2.3% to Σ^0 and 9.4% to Λ [16], which further lessens the role of the Σ^0 to the formation of $m_{\Lambda d}$ in the range of interest. Thus, the excitation and decay of intermediate Σ^0 's is neglected in the present analysis.

Λd pairs may also be produced by multi-step processes such as (4) where the negative kaon is absorbed by a single nucleon $K_{stop}^- N[A-1] \rightarrow \Lambda \pi[A-1]$ followed by a pion final state interaction (FSI) $\pi[A-1] \rightarrow d[A-3]$, or (5) where a K_{stop}^- is absorbed by a pair of nucleons $K_{stop}^- NN[A-2] \rightarrow \Lambda N[A-2]$ and a N pick-up reaction $N[A-2] \rightarrow d[A-3]$ follows. Both processes were modeled by constraining the interacting N and NN nucleons to obey Fermi motion. In the multi-step process (4), the momentum of Λ 's (p_Λ) is below 250 MeV/c, while the measured p_Λ is in the range ≈ 450 -700 MeV/c. Kinematic constraints also disfavor process (5); in fact, the phase space of $|\vec{p}_\Lambda + \vec{p}_d|$ vs $m_{\Lambda d}$ of (5) only slightly overlaps the experimental data.

The smooth behavior of reaction channels (1) $\Lambda d n n p$, (2) $\Lambda d n d$ and (3) $\Lambda d t$ is unable to explain the structure of the bump at the tail of the measured $m_{\Lambda d}$ distribution. To obtain its position ($m_{\Lambda d}$), width ($\Gamma_{\Lambda d}$) and yield ($Y_{\Lambda d}$), the Λd invariant mass distribution was fitted to a linear combination of the following distributions: the phase space of channels (1), (2) and (3), and a Gaussian function (G) whose parameters are left free. The result is the big-dot curve which overlaps the full-line curve when the Gaussian strength is set to zero. In this approach, the events underneath the full-line curve are the background events. Finally, the Gaussian distribution is represented by the grey-fill curve whose parameters are $m_{\Lambda d}=3251 \pm 6$ MeV/c², $\Gamma_{\Lambda d}=36.6 \pm 14.1$ MeV/c² and $Y_{\Lambda d}=(4.4 \pm 1.4) \times 10^{-3}/K_{stop}^-$. Indeed, the quoted $\Gamma_{\Lambda d}$ is the intrinsic width of the bump which, when summed in quadrature with the bin width ($\sigma_{bin}=5.8$ MeV/c²) and spectrometer resolution, ($\sigma_{\Lambda d}=6.0$ MeV/c²), yields the full width of the Gaussian distribution.

When the experimental data are fitted to a linear combination of only (1), (2) and (3) phase spaces (curve not shown), the chi-square (χ_{123}^2) is 7.61 with 5 degrees of freedom. The inclusion of G yields $\chi_{123G}^2=0.17$ with 2 degrees of freedom. Since $\chi_{123}^2/5 \gg \chi_{123G}^2/2$, the additional term G significantly improves the goodness of the fitting. A measure of this improvement is given by the F test for validity of adding the G term, where $F = \frac{2}{3}(\chi_{123}^2 - \chi_{123G}^2)/(\chi_{123G}^2)$. In this case $F=29.2$. This large value of F ensures a confidence level slightly above 95% in the relative merit of the G term [17].

The statistical significance \mathcal{Z} of the $m_{\Lambda d}=3250$ MeV/c² signal is evaluated by using the Uniformly Most Powerful test among the class of Unbiased tests (UMPU) method, which is described in Ref.[18]. In this scheme, the total number of events observed around the bump is evaluated at 3σ . In the same 3σ interval, the number of background events is accounted for by the number of events below the full-line curve. The resulting statistical significance is $\mathcal{Z}_{3\sigma}=3.9$.

The $\cos\Theta_{\Lambda d}$ distribution of these bump events falling in the mass interval $3220 \leq m_{\Lambda d} \leq 3280$ MeV/c² is shown in the inset of Fig. 3. The distribution peaks at $\cos\Theta_{\Lambda d}=-1$ and spans a few bins above it. Its narrow width indicates that the Λd events arise from slowly-moving clusters. This is corroborated by the momentum distribution of Λd pairs ($p_{\Lambda d}$) in the mass range of the

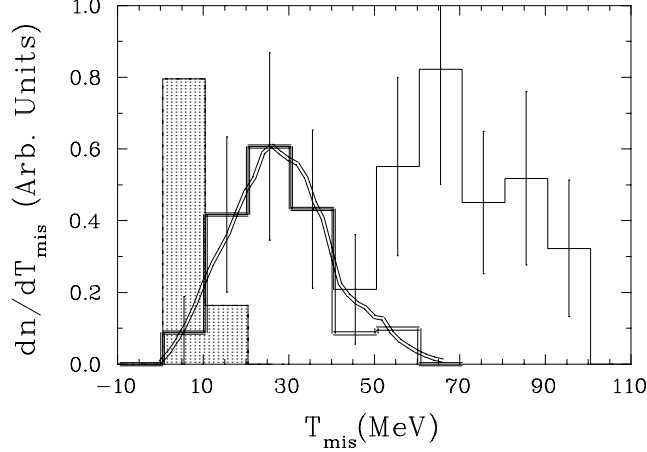


Fig. 4. Missing kinetic energy distribution of the ${}^6\text{Li}(K_{stop}^-, \Lambda d)nd$ reaction (thin-line histogram). Thick-line histogram, T_{mis} distribution for events correlated to the $m_{\Lambda d}=3250\pm 30$ MeV/ c^2 mass range. Thick-line curve, simulated missing kinetic energy distribution of the undetected nd pairs with the energy of the spectator deuteron below 4 MeV. The curve is normalized to the thick-line experimental data. Grey-fill histogram, simulated T_{mis} distribution for the ${}^6\text{Li}(K_{stop}^-, \Lambda d)t$ reaction correlated to the $m_{\Lambda d}=3250\pm 30$ MeV/ c^2 mass interval. The histogram is arbitrarily normalized to the data. More details are given in the text.

bump (figure not shown), the average value of which is about 190 MeV/ c (4.7 MeV), which corresponds to a particle with $m_{\Lambda d}=3251$ MeV/ c^2 moving with a $\beta=0.058$. Below the bump region $m_{\Lambda d} \leq 3220$ MeV/ c^2 , the $\cos\Theta_{\Lambda d}$ distribution (figure not shown) is still peaked at -1 but with a FWHM about 4 times broader than the $\cos\Theta_{\Lambda d}$ distribution of the bump events.

In the study of ${}^6\text{Li}$, the Λd channel leaves an undetected $3N$ system which can be a t , nd or nnp in the reaction final state. For nd , the missing kinetic energy distribution (dn/dT_{mis}) can be determined by means of the equation $T_{mis} = (m_{K_{stop}^-} + m_{{}^6\text{Li}} - m_{\Lambda} - m_n - 2m_d) - (T_{\Lambda} + T_d)$, where $(T_{\Lambda} + T_d)$ is the sum of the kinetic energies of the detected particles, and m is the mass of a generic particle. The measured distribution of the missing kinetic energy is shown in Fig. 4 (thin-line histogram). It is shown only in the region up to 100 MeV where intensities are more accurately known. There is a bump in the kinetic energy distribution at around 25 MeV which is strongly correlated to the 3250 MeV/ c^2 bump of Fig. 3; in fact, a $3220 \leq m_{\Lambda d} \leq 3280$ MeV/ c^2 constraint produces the thick-line histogram of Fig. 4. Such an occurrence can be explained by assuming the absorption process to start with the $\alpha(K_{stop}^-, \Lambda d)n$ reaction, where α is a substructure of ${}^6\text{Li}(\equiv \alpha + d_H)$ [8]. The d_H deuteron of ${}^6\text{Li}$ is assumed to participate in the transition only by obeying the Hulthen momentum distribution [19] which lies between 0 and 150 MeV/ c being peaked at about 50 MeV/ c . To account for the kinematics of the full reaction, the simulated distributions of Λd events are shaped to fit the measured distributions in the ranges $p_{\Lambda, d}=600\pm 150$ MeV/ c , $3220 \leq m_{\Lambda d} \leq 3280$ MeV/ c^2 and $-1 \leq \cos\Theta_{\Lambda d} \leq -0.9$. The result of these simulations is the thick-line curve in Fig. 4, which is normalized to the thin-line experimental data. The curve follows closely the behavior of the data, which supports the assumption that the initial stage of the reaction is the $K_{stop}^- \alpha$ -cluster absorption, and most of the kinetic energy is taken away by the undetected neutrons.

For the ${}^6\text{Li}(K_{stop}^-, \Lambda d)t$ reaction, the simulated dn/dT_{mis} distribution is represented by the grey-fill histogram, which is arbitrarily normalized to the data. The constraint $3220 \leq m_{\Lambda d} \leq 3280$ MeV/c² requires tritons to peak at about 10 MeV kinetic energy. Such a peak does not appear in the experimental missing kinetic energy distribution, denoting that only limited strength is available to the Λdt channel. As well, the $\Lambda dppn$ channel plays little part in building the 25 MeV bump because of its negligible strength in the $m_{\Lambda d}=3250 \pm 30$ MeV/c² mass interval (i.e. dashed-line curve of Fig. 3). As a final comment, $\Sigma^0 \rightarrow \Lambda\gamma$ decays can only feed the high-energy region of the T_{mis} spectrum since the undetected γ -rays take away 74 MeV.

The method employed to analyze the K^- absorption in ${}^6\text{Li}$ was also employed to analyze the ${}^{12}\text{C}(K_{stop}^-, \Lambda d)A'$ data. In general, these data are spread over a larger angular interval; for instance, compare the distribution of Fig. 3 inset with that of Fig. 5 inset. This behavior is probably due to $\Lambda - A'$ and $d - A'$ final state interactions (FSI); in fact, FSI for ${}^6\text{Li}$ are smaller than for ${}^{12}\text{C}$ since the residual nucleus is simply a deuteron. Fig. 5 shows the distribution of the Λd invariant mass of ${}^{12}\text{C}$. The high-energy part resembles a shoulder in shape, which cannot be uniquely fit with a Gaussian distribution as was done for ${}^6\text{Li}$. The $\cos\Theta_{\Lambda d}$ distribution for the $3220 \leq m_{\Lambda d} \leq 3280$ MeV/c² events is reported in the inset of Fig. 5. This distribution, as well as the similar distribution for ${}^6\text{Li}$ (inset of Fig. 3), is peaked at around -1 although now it has a larger width. The $m_{\Lambda d}$ behavior was also examined for $\cos\Theta_{\Lambda d} \leq -0.9$, the same angular range as ${}^6\text{Li}$. However, the data do not display any evident bump-like structure.

IV. DISCUSSION

The results were obtained by comparing the behavior of three observables; i.e., $m_{\Lambda d}$, $\cos\Theta_{\Lambda d}$ and $T_{\Lambda d}$ the last two being independently measured. The ${}^6\text{Li}$ measurements provided results

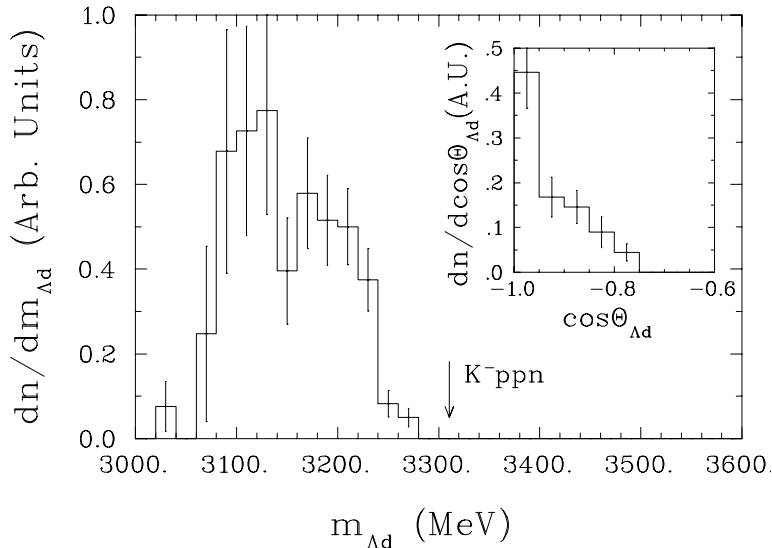


Fig. 5. Invariant mass distribution of Λd pairs from the ${}^{12}\text{C}(K_{stop}^-, \Lambda d)A'$ reaction. Inset, $\cos\Theta_{\Lambda d}$ distribution when the invariant mass of the Λd pairs is cut between 3220 and 3280 MeV/c².

of primary interest in the $m_{\Lambda d}=3250\pm 30$ MeV/c² mass range whose interpretation required extensive modeling. The ¹²C data appear to be affected by FSI, which partially screens the underlying physics.

For kaon absorption in ⁶Li, reaction kinematics were required to feed both the 3250±30 MeV/c² mass range and the correlated 25±25 MeV kinetic energy range. The Λdnd reaction channel meets these requirements along with a moderate $\Lambda dnnp$ contribution. The monotonic behavior of the Λdnd and $\Lambda dnnp$ phase spaces in the mass interval 3250±30 MeV/c² cannot explain the bump structure. Both the Λdt channel and the $\Sigma^0 \rightarrow \Lambda\gamma$ decay bring a negligible strength in the $m_{\Lambda d}=3250\pm 30$ MeV/c² interval, whereas multistep processes are disfavoured by the reaction kinematics. Therefore, the symmetric shape of the bump was fit with a Gaussian distribution, which yields $m_{\Lambda d}=3251\pm 6$ MeV/c², $\Gamma_{\Lambda d}=36.6\pm 14.1$ MeV/c² and $\mathcal{Z}_{3\sigma}=3.9$. Since the bump at about 3140 MeV/c² is probably an artifact due the poor statistics along with the low acceptance of the apparatus, it cannot be compared with a similar structure at $m_{\Lambda d}=3160$ MeV/c² obtained by the FOPI collaboration in heavy ion measurements [21].

Extensive $K_{stop}^- {}^6Li \rightarrow \Lambda dnd$ modeling which relied on the cluster structure of lithium, ${}^6Li(\equiv \alpha + d_H)$ [8] was required to describe the $T_{mis}=25$ MeV bump (Fig. 4). In fact, a reaction mechanism capable of explaining the bump requires that negative kaons are preferentially absorbed by α -like substructures, $K_{stop}^- \alpha \rightarrow [K^- ppn] + n$, while the d_H deuterons participate in these processes as spectators. Final state neutrons remove the excess energy. In these dynamics, neutrons are the *spectroscopy particles* of the $[K^- ppn]$ cluster formation. The $[K^- ppn]$ clusters finally decay via the $[K^- ppn] \rightarrow \Lambda d$ channel. Λ -hyperons and deuterons are observed to have a strong angular correlation at around 180°. In this measurement, other decay channels were not examined.

$[K^- 3N]$ clusters were discussed earlier in the framework of \bar{K} nuclear bound states. The nuclear ground state of $[K^- \otimes {}^3He + \bar{K}^0 \otimes {}^3H]$ was predicted to be 108 MeV deep and 20 MeV wide [3]. Similar quantities can be determined by assuming $[\bar{K} ppn] \equiv [K^- \otimes {}^3He + \bar{K}^0 \otimes {}^3H]$, such as the $[K^- ppn]$ binding energy $B_{K^- ppn} = (m_{K^-} + 2m_p + m_n) - m_{\Lambda d} = 58\pm 6$ MeV and $\Gamma_{\Lambda d}=36.6\pm 14.1$ MeV/c², where m is the generic particle rest mass. Although the theoretical predictions agree with experiments supporting formation of kaonic nuclear states, the agreement is poor. A comment on the binding energy and width is worthy of note. The values of B and Γ depend on the bump position and width, respectively. In this measurement, the bump develops close to the phase space endpoint of the ${}^6Li(K_{stop}^-, \Lambda d)nd$ reaction (3280 MeV, see Fig. 3), which might modify the structure of the bump thus $B_{K^- ppn}$ and $\Gamma_{\Lambda d}$.

A recent study of the $K_{stop}^- A \rightarrow \Lambda p A'$ reaction, where A combines 3 targets ⁶Li, ⁷Li and ¹²C [1], found evidence of a kaon bound state $[K^- pp]$. The binding energy $B_{K^- pp}= 115$ MeV and the decay width $\Gamma_{\Lambda p}=67$ MeV/c² were determined from the Λp invariant mass distribution. For the case of the Λp measurement, both parameters B and Γ are larger than our results. The result seems to contradict a theoretical expectation for small binding energy to be correlated with

large decays widths. In view of these results, further theoretical and experimental developments are needed. The existence of bound kaonic states in nuclei remains controversial [4,6,22], and needs to be definitively settled.

The present analysis indicates an alternative way to detect $[\overline{K}ppn]$ cluster decays when forming in ${}^4\text{He}$ or ${}^6\text{Li}$. Formation of these clusters is accompanied by neutrons whose kinetic energy is below 50 MeV. If the role of FSI is marginal, these neutrons should peak at around 25 MeV (Fig. 4 thick-line). For ${}^{12}\text{C}$, such a distinctive pattern disappears (spectrum not shown) probably being engulfed by the continuum. Proposals to use the (K, n) reaction to search for strange heavy baryons[20] should account for these results.

V. CONCLUSIONS

We report in this letter the results of a kaon absorption study by means of the $K_{stop}^- A \rightarrow \Lambda d A'$ reaction; the nuclei examined were ${}^6\text{Li}$ and ${}^{12}\text{C}$. The experiment was performed with the FINUDA spectrometer, which was installed at the DAΦNE ϕ -facility (LNF). The study makes full use of the capability of FINUDA to reconstruct the tracks of most particles involved in the absorption reaction with the exception of the residual nucleus. The analyses deal with correlated particle pairs Λd , which considerably clean the spectra from accidental events.

For light nuclei, the K^- absorption reaction presents some common features: (1) The $m_{\Lambda d}$ distribution develops its strength well below the sum of the K^-, p, p, n rest masses (denoted with an arrow in Figs. 3 and 5). (2) A strong angular correlation exists between Λ hyperons and deuterons; in fact, the $\Theta_{\Lambda d}$ distribution results are sharply peaked at around 180° .

In ${}^6\text{Li}$, a bump was found at the tail of the $m_{\Lambda d}$ distribution with a peak at 3251 ± 6 MeV/ c^2 , a width 36.6 ± 14.1 MeV/ c^2 , and a yield of $(4.4 \pm 1.4) \times 10^{-3} / K_{stop}^-$ with a statistical significance 3.9. The combined picture of the opening angle distribution of the detected Λd pairs and their momentum distribution shows that the Λd events are emitted from $[K^-ppn]$ slow-moving clusters. The cluster momentum is counterbalanced by $T_n < 50$ MeV neutrons. The corresponding $[K^-ppn]$ binding energy is $B_{K^-ppn} = 58 \pm 6$ MeV. In the case of ${}^{12}\text{C}$, a shoulder structure replaced the bump in the ${}^6\text{Li}$ Λd invariant mass spectrum. An analysis based on statistical methods does not yield a unique set of $m_{\Lambda d}$ (B_{K^-ppn}) and $\Gamma_{\Lambda d}$ parameters.

The values of $B_{K^-ppn} \sim 58$ MeV and $\Gamma_{K^-ppn} \sim 37$ MeV/ c^2 obtained for the $[\overline{K}ppn]$ bound system can be compared to the values of an earlier theoretical work [3] based on the possible existence of \overline{K} bound nuclear states. Based on a ground state of $[K^- \otimes {}^3\text{He} + \overline{K}^0 \otimes {}^3\text{H}]$, $B_{K^-} = 108$ MeV and $\Gamma_{K^-} = 20$ MeV. However overall agreement is poor and improved calculations are needed, especially now that the present result is consistent with the formation of a bound $[K^-ppn]$ cluster, and the reaction mechanism for neutrons has been deduced. Increasing theoretical interest in obtaining a reliable physical framework for analysis of recent data

is evidenced by the number of recent publications [22,23,24,25,26].

References

- [1] M. Agnello et al., Phys. Rev. Lett. **94** (2005) 212303.
- [2] M. Iwasaki et al., arXiv:nucl-ex/0310018v2 Nov. 2004;
T. Suzuki et al., Nucl. Phys. **A754** (2005) 375c.
Neutrons from the $K_{stop}^- {}^4He \rightarrow nA'$ reaction were recently measured at *KEK*, and the results presented by H. Yim at the IX International Conference on Hypernuclear and Strange Kaon Physics, 10-14 Oct. 2006, Mainz (Germany). A narrow (≈ 21 MeV) bump structure was not observed in the neutron spectrum. However, the analyses are not yet finalized (M. Iwasaki's, private communication).
- [3] Y. Akaishi and T. Yamazaki, Phys. Rev. **C65** (2002) 044005;
A. Doté, Y. Akaishi and T. Yamazaki, Nucl. Phys. **A738** (2004) 372;
Y. Akaishi, A. Dote' and T. Yamazaki, Phys.Lett. **B613** (2005) 140.
- [4] E. Oset and H. Toki, Phys. Rev. **C74** (2006) 015207.
- [5] E. Friedman, A. Gal and C.J. Batty, Phys. Lett. **B308** (1993) 6;
E. Friedman, A. Gal and C.J. Batty, Nucl Phys. **A579** (1994) 518;
E. Friedman, A. Gal, J. Mareš and A. Cieply, Phys. Rev. **C60** (1999) 0243146.
- [6] A. Baca, C. Garcia-Recio and J. Nieves, Nucl. Phys. **A673** (2000) 335;
A. Cieply, E. Friedman, A. Gal and J. Mareš and Nucl. Phys. **A696** (2001) 173.
- [7] T. Suzuki et al., Phys. Lett. **B597** (2004) 263.
The existence of the strange tribaryon $S^0(3115)$ was recently withdrawn by M. Iwasaki; i.e., his contribution to the IX International Conference on Hypernuclear and Strange Kaon Physics, 10-14 Oct. 2006, Mainz (Germany).
- [8] M. Agnello et al, Nucl. Phys. **A775** (2006) 35.
- [9] M. Agnello et al., Phys. Lett. **B622** (2005) 35.
- [10] M. Agnello et al., *FINUDA, a detector for Nuclear Physics at DAΦNE*, LNF Internal Report, LNF-93/021(IR), 1993;
M. Agnello et al., *FINUDA, Technical Report*, LNF Internal Report, LNF-95/024(IR), 1995.
- [11] V. Filippini, M. Marchesotti, and C. Marciano, Nucl. Instr. and Methods **A424** (1999) 343.
- [12] P. Bottan et al., Nucl. Instr. and Methods **A427** (1999) 423;
P. Bottan et al., Nucl. Instr. and Methods **A435** (1999) 153.
- [13] M. Agnello et al., Nucl. Instr. and Methods **A385** (1997) 58.
- [14] L. Benussi et al., Nucl. Instr. and Methods **A361** (1995) 180;
L. Benussi et al., Nucl. Instr. and Methods **A419** (1998) 648.

- [15] A. Pantaleo et al., Nucl. Instr. and Methods **A545** (2005) 593.
- [16] P. A. Katz, K. Bunnell, M. Derrick, T. Fields, L. G. Hyman and G. Keyes, Phys. Rev. **D1** (1970) 1267.
- [17] P. R. Bevington, Data Reduction and Error Analysis for the Physical Sciences, McGraw-Hill Book Company. The F test is discussed in Section 10-2.
- [18] Lehman, Testing Statistical Hypotheses, 2nd edition, Wiley (1986);
J. T. Linnemann, arXiv:physics/0312059v2 Dec. 2003.
- [19] S.Barbarino et al., Phys. Rev. **C21** (1980) 1104.
- [20] T. Kishimoto, Phys. Rev. Lett. **83** (1999) 4701;
T. Kishimoto et al., Nucl. Phys. **A754** (2005) 383c.
- [21] N.Herrmann, Proc. EXA05 Conference, Vienna 2005, ISBN 3-7001-3616-1, p. 73.
- [22] J. Mareš, E. Friedman and A. Gal, Nucl. Phys. **A770** (2006) 84;
On the same topic, J. Mareš, E. Friedman and A. Gal, Phys. Lett. **B606** (2005) 295.
- [23] X. Z. Zhong, L. Li, G. X. Peng and P. Z. Ning, Phys. Rev. **C74** (2006) 034321.
- [24] A. Doté, H. Horiuchi, Y. Akaishi and T. Yamazaki, Phys. Lett. **B590** (2004) 51;
A. Doté, Y. Akaishi and T. Yamazaki, Nucl. Phys. **A738** (2004) 327;
A. Doté, Y. Akaishi and T. Yamazaki, Nucl. Phys. **A754** (2005) 391c.
- [25] A. N. Ivanov, P. Kienle, J. Marton and E. Widmann, arXiv:nucl-th/0512037v1 Dec. 2005.
- [26] W. Weise, nucl-th/0701035v1, to appear on Eur. Journ. of Phys. See also references therein quoted.